



# An equivalent method for optimization of particle tuned mass damper based on experimental parametric study

Zheng Lu <sup>a,b</sup>, Xiaoyi Chen <sup>b</sup>, Ying Zhou <sup>a,b,\*</sup>



<sup>a</sup> State Key Laboratory of Disaster Reduction in Civil Engineering, Tongji University, Shanghai 200092, China  
<sup>b</sup> Research Institute of Structural Engineering and Disaster Reduction, Tongji University, Shanghai 200092, China

## ARTICLE INFO

### Article history:

Received 18 February 2017

Received in revised form 15 April 2017

Accepted 27 May 2017

Available online 12 October 2017

Handling Editor: L. G. Tham

### Keywords:

Particle tuned mass damper

Tuned mass damper

Particle damper

Passive control

Equivalent principle

Filling ratio

Optimization design

## ABSTRACT

A particle tuned mass damper (PTMD) is a creative combination of a widely used tuned mass damper (TMD) and an efficient particle damper (PD) in the vibration control area. The performance of a one-storey steel frame attached with a PTMD is investigated through free vibration and shaking table tests. The influence of some key parameters (filling ratio of particles, auxiliary mass ratio, and particle density) on the vibration control effects is investigated, and it is shown that the attenuation level significantly depends on the filling ratio of particles. According to the experimental parametric study, some guidelines for optimization of the PTMD that mainly consider the filling ratio are proposed. Furthermore, an approximate analytical solution based on the concept of an equivalent single-particle damper is proposed, and it shows satisfied agreement between the simulation and experimental results. This simplified method is then used for the preliminary optimal design of a PTMD system, and a case study of a PTMD system attached to a five-storey steel structure following this optimization process is presented.

© 2017 Elsevier Ltd. All rights reserved.

## 1. Introduction

How to increase the structural safety and reliability under dynamic loads, such as earthquakes, winds, impacts, etc., which may cause excessive responses of the structure and discomfort feelings of the occupants, has always been an important issue in civil engineering area. The disaster reduction theory [1] has advanced from increase of structural resistance by strengthening the elements and material, to dissipation or insulation of the input energy by technological innovations. The theory of energy absorption that was initially proposed by Kelly and Skinner [2] has many practical applications in modern society, which was mainly achieved by attaching auxiliary devices, such as energy dissipation braces, damping outrigger systems [3], dampers [4–7], or exerting external energy inputs, etc., to adjust the dynamic characteristics of the structure and thus control the responses.

According to the state of external energy supply, the vibration control can be categorized as passive control, active control, hybrid control and semi-active control, among which the passive control has wide applications due to its simple concept and mechanism. The tuned mass damper (TMD) [8], a typical passive control device with the advantages of simple characteristics, convenient installation, low cost and favorable control effects under specific tuning frequency, has been widely researched and applied in tall and slender structures to reduce the responses, such as high-rise buildings [9], wind turbine towers [10],

\* Corresponding author. State Key Laboratory of Disaster Reduction in Civil Engineering, Tongji University, Shanghai 200092, China.

E-mail addresses: [luzheng111@tongji.edu.cn](mailto:luzheng111@tongji.edu.cn) (Z. Lu), [sducxy@163.com](mailto:sducxy@163.com) (X. Chen), [yingzhou@tongji.edu.cn](mailto:yingzhou@tongji.edu.cn) (Y. Zhou).

and pedestrian bridges [11]. Tanaka and Mark [12] conducted a parametric study of the TMD based on the aero-elastic wind tunnel test of a 1/1000 scale model of the CAARC Standard Tall Building to investigate its efficiency in suppressing the wind-induced vibrations. However, the narrow bands of the suppression frequency, ineffective reduction for non-stationary vibrations and sensitivity problems owing to mistuning limit the vibration control effects of the TMDs. According to Clinton [13], the TMDs were sensitive to surrounding environment, such as wind velocity, temperature, relative humidity and the type of earthquakes.

The particle damper (PD), a new type of passive control device that makes an improvement based on the traditional impact damper, utilizes both momentum transfer and energy dissipation achieved by collisions among particles, collisions between particles and the container wall, friction and sound radiation to attenuate the vibration [14]. The particle damper, which has wide reduction frequency bands, ruggedness, reliability, insensitivity to extreme temperatures and causes slight changes to the primary structure, has attracted many scholars to study on its damping performance [15–17]. However, compared to the relatively mature design processes of the TMDs, inherent puzzlements regarding to the working mechanism of the particle dampers are still remained.

Considering the advantages and limitations of both TMDs and PDs, a combinative damper - particle tuned mass damper (PTMD), is generated by suspending a multiple particle damper on the top of a structure, which can broaden the suppression frequency bands through collisions and thus improve the reduction efficiency and durability. Yan et al. [18] experimentally investigated the vibration reduction effects of a tuned particle damper attaching to a viaduct system under seismic loads and founded that the suppression frequency band was wider than that of the TMDs; Lu et al. [19,20] performed an aero-elastic wind tunnel test on a reduced-scale Benchmark model attached with a PTMD and analyzed the influence of some parameters, such as auxiliary mass ratio, particle density, mass ratio of container to particles and wind velocity, on the vibration control effects for wind-excited responses of high-rise buildings.

Actually, the PTMD introduces the nonlinear damping into the linear TMD within the concept of nonlinear energy sink (NES) in order to transfer the energy from the primary structure to the nonlinear damping devices and dissipate it. The NES usually has nonlinear stiffness or nonlinear damping to widen the band of resonant frequencies. In addition, the NES has the function of target energy transfer and dissipation to alternate the energy distribution in space and frequency. For example, Roberson [21] proposed a nonlinear dynamic vibration absorber by attaching a secondary system by means of a spring whose load-deflection characteristics was sum of a linear and cubic term, which proved to be capable of dissipating energy in a wider range of frequencies than the traditional linear TMDs under earthquakes. Spencer [22,23] founded that the responses of a nine-storey structure attached with a NES could be significantly and quickly reduced under seismic and explosion inputs through shaking table tests and field tests, and the NES was efficacious in a wide range of frequencies.

Up till now, the research on the PTMD is in the early stage, especially for the theoretical and numerical study. The core issue to evaluate the damping performance of the PTMD is still the numerical simulation of the highly nonlinear behavior of particles. Papalou and Masri [24] proposed an approximate analytical solution by equating the multi-unit particle damper to a single-unit impact damper based on certain equivalent principles and shown that this method can provide an adequate estimate of the structural responses when the damper was operating in the vicinity of the optimum range of parameters; Xia et al. [25] proposed a coupling simulation algorithm for the particle damper based on the discrete element method and finite element method, and the analytical and experimental results were compared; Lu et al. [26] numerically investigated the performance of both vertical and horizontal particle dampers under different dynamic loads by using discrete element method and used the concept of *Effective Momentum Exchange* to characterize the underlying physics of operating particle dampers; Lu et al. [27] further established a high-fidelity simulation process to account for all significant interactions among the particles and with the host structure system based on the modified discrete element method; Wang and Wu [28] developed a novel simulation method based on multiphase flow theory of gas particle to study the vibration characteristics of a cantilever rectangular plate with particle dampers, and the numerical predictions agreed well with the experimental results. Moreover, Sanchez and Carlevaro [29] conducted a nonlinear dynamic analysis of a single-degree-of-freedom (SDOF) mechanical model with a particle damper, and the optimum gap size for the best performance of granular damping was obtained.

However, further study to understand the underlying physical mechanics of the PTMD is necessary and there are scarcely guidelines for optimization design of the particle dampers for now. In this paper, free vibration tests and shaking table tests are carried out to investigate the damping performance of the PTMD. The influencing principles of some key parameters are discussed, through which the guidelines for the optimization of the PTMD can be concluded. A simplified analytical solution by equating the PTMD to a single-particle damper is presented and proves to have the reasonability and accuracy in estimating the vibration control effects of the PTMD. Furthermore, a convenient procedure on the preliminary design of a PTMD by using the proposed equivalent method is put forward and shows the optimal vibration reduction effects through a case study of applying the PTMD to a five-storey steel structure.

## 2. Experimental investigation

### 2.1. Experimental setup

The main structure in the experiment is a one-storey steel frame structure, as shown in Fig. 1(a). Its dimensions are 320 mm × 110 mm × 500 mm, and the mass is 1.6 kg. The lateral stiffness in the longitudinal direction is 500 N/m. An additional

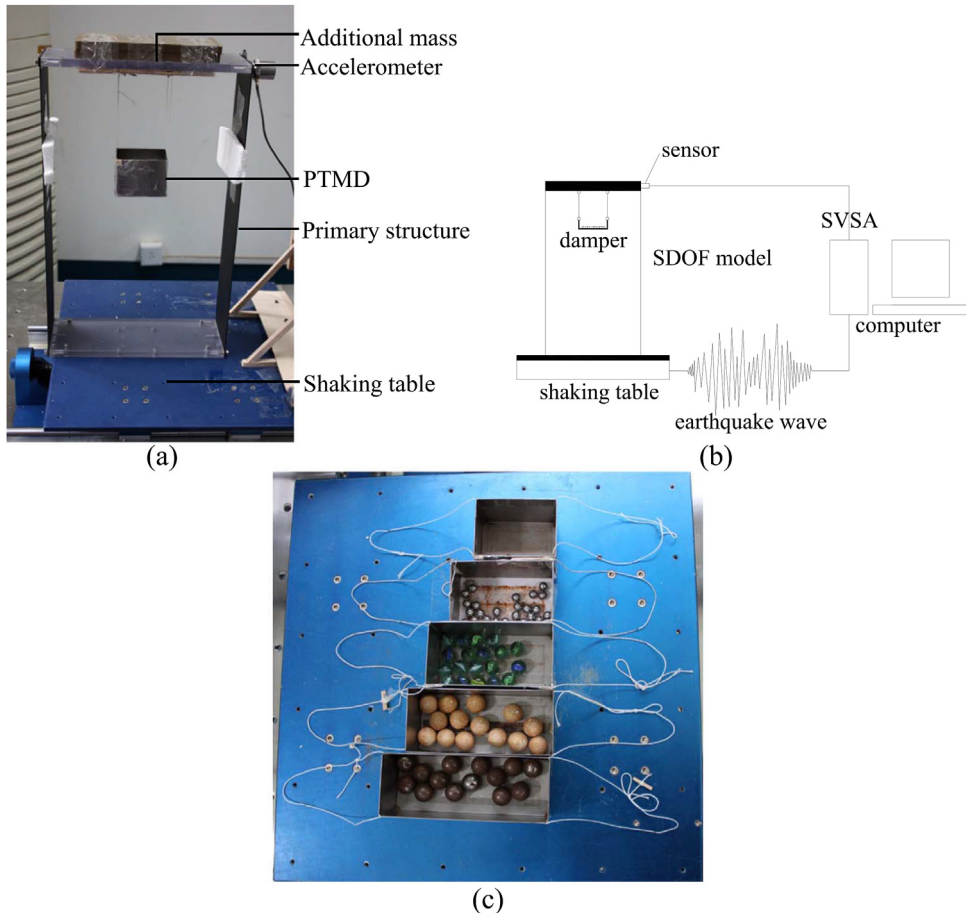


**Fig. 1.** Test model information: (a) Experimental model; (b) schematic diagram of the experiment; (c) various types of PTMD.

mass of 6 kg is attached on its top to finally adjust the natural frequency to 1.37 Hz, which is close to the common frequency of high-rise buildings. The particle tuned mass damper is composed of a container filled with particles, which is suspended by four vertical strings with the same length from the top of the structure. The cable length is 13 cm.

The cross sections of five containers are kept the same as 60 mm × 60 mm, whereas the lengths can be changed as 80 mm, 100 mm, 120 mm, 140 mm and 160 mm. Four kinds of particles, including glass balls with 15 mm diameter, ceramic balls with 20 mm diameter, stainless steel balls with 10 mm diameter and steel balls with 20 mm diameter, are used. Different types of containers and particles are shown in Fig. 1(b). It is also interesting to compare the vibration reduction effects of the PTMD and the TMD. Therefore, in some cases, the particles are fixed on the container to act as the TMD for comparison.

Different levels of seismic waves, including El Centro wave (1940, NS), Kobe wave (1995, NS), and Shanghai artificial wave (SHW2, 1996), are applied in the experiment. In addition, the displacement and acceleration on the top of the structure are obtained by the laser displacement sensor (IL-300), accelerometer and structure vibration signal acquisition and analysis system (SVSA), respectively.

## 2.2. Vibration reduction effects of PTMD

To obtain the frequency characteristics of the test structure under different cases and form a preliminary understanding of the damping performance of the PTMD, free vibration tests are carried out. For example, when the length of the container is 80 mm and the initial displacement is 2 cm, the comparison of the acceleration time histories of the structure attaching with a TMD whose mass is about 128 g, with a PTMD having the same mass, without dampers is shown in Fig. 2(a). It can be found that the responses of the controlled structure are much smaller than those of the uncontrolled structure. Furthermore, the acceleration attenuation rate in the case of the PTMD is much higher than that in the case of the TMD.

Fig. 2(b) shows the corresponding fast Fourier transform of acceleration responses. It can be observed that there is only one peak of the frequency response curve in the case of the uncontrolled structure, which is approximately 1.4 Hz, corresponding to the natural frequency of the SDOF test frame, and the magnitude of this primary motion mode is very high. In the

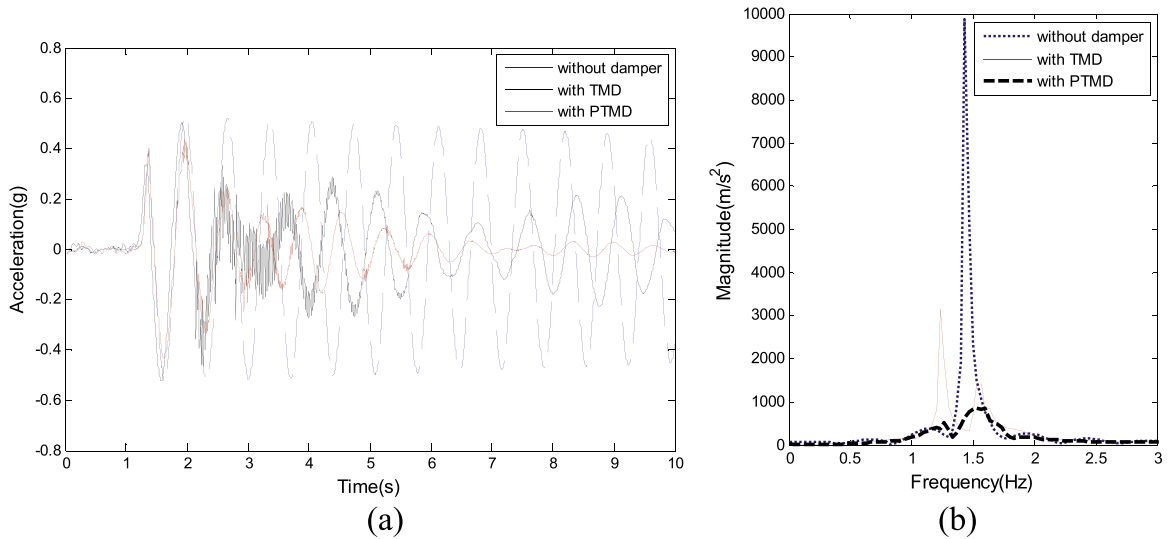


**Fig. 2.** Responses of the test structure with a PTMD/with a TMD/without dampers: (a) acceleration time history; (b) fast Fourier transform of acceleration response.

case of the TMD, the response frequency curve has two peaks, which locate at both sides of 1.4 Hz, representing the motion modes dominated by the structure and the TMD, respectively. The magnitudes are much less than that of the uncontrolled structure, suggesting that the input energy has been partly transferred to the attached TMD.

In the case of the PTMD, the curve has two much lower peaks, in which the first peak can be negligible and the second peak is also very small, suggesting that the vibration energy is mainly concentrated on the PTMD; thus, it can prevent the main structure from severe vibrating. Additionally, the second vibration mode, whose motion directions of the container and the main structure are opposite, has more advantages than the first vibration mode. The mass dampers take advantages of this anti-phase movement between the damper and the main structure so that they can significantly reduce the vibration.

### 3. Experimentally parametric analysis

To optimize the PTMD and develop a practical way to design the PTMD, a series of shaking table tests are carried out and the influence of following system parameters on the vibration control effects is investigated: filling ratio of particles, auxiliary mass ratio and particle density.

Although the acceleration peak value is an important controlling index in structure design, it only shows the structural dynamic response at a certain instant. However, the root-mean-square (r.m.s) value is an indicator of the vibration energy, which reflects the responses on a whole time period. Therefore, the r.m.s value of the acceleration response is chosen to evaluate the damping performance of the PTMD. The vibration attenuation rate is defined as follow:

$$\text{Attenuation rate} =$$

$$\frac{(\text{acceleration r.m.s of uncontrolled structure} - \text{acceleration r.m.s of controlled structure})}{\text{acceleration r.m.s of uncontrolled structure}}$$

#### 3.1. Effects of filling ratio of particles

In addition to the added mass for tuning frequency, the PTMD mainly dissipates the vibration energy by collisions among particles and collisions between particles and the container. The parameter that is closely related to the colliding degree is the filling ratio of particles, which is defined as the ratio between the particle amount and the maximum particle amount available in one layer of the container. In the experiment, this parameter is designed to be not more than 100% in order to avoid the piling up situation, which would otherwise limit the sufficient movement of particles and negatively affect the energy dissipation. The influence of the filling ratio of particles on the damping performance of the PTMD is examined by using different lengths of containers while keeping the total auxiliary mass ratio and the seismic inputs (El Centro wave (0.15 g)) the same.

By changing the diameter, number and material type of particles, the auxiliary mass ratio of particles to the primary structure ( $\mu$ ) can be changed as 0.5%, 1.5%, 2% and 4%. Based on the current experimental test data, the corresponding filling ratio of particles can be computed. Fig. 3 plots the effects of the filling ratio of particles on the attenuation rate of both r.m.s and peak acceleration in those cases of mass ratios. It can be observed that the filling ratio of particles can significantly affect

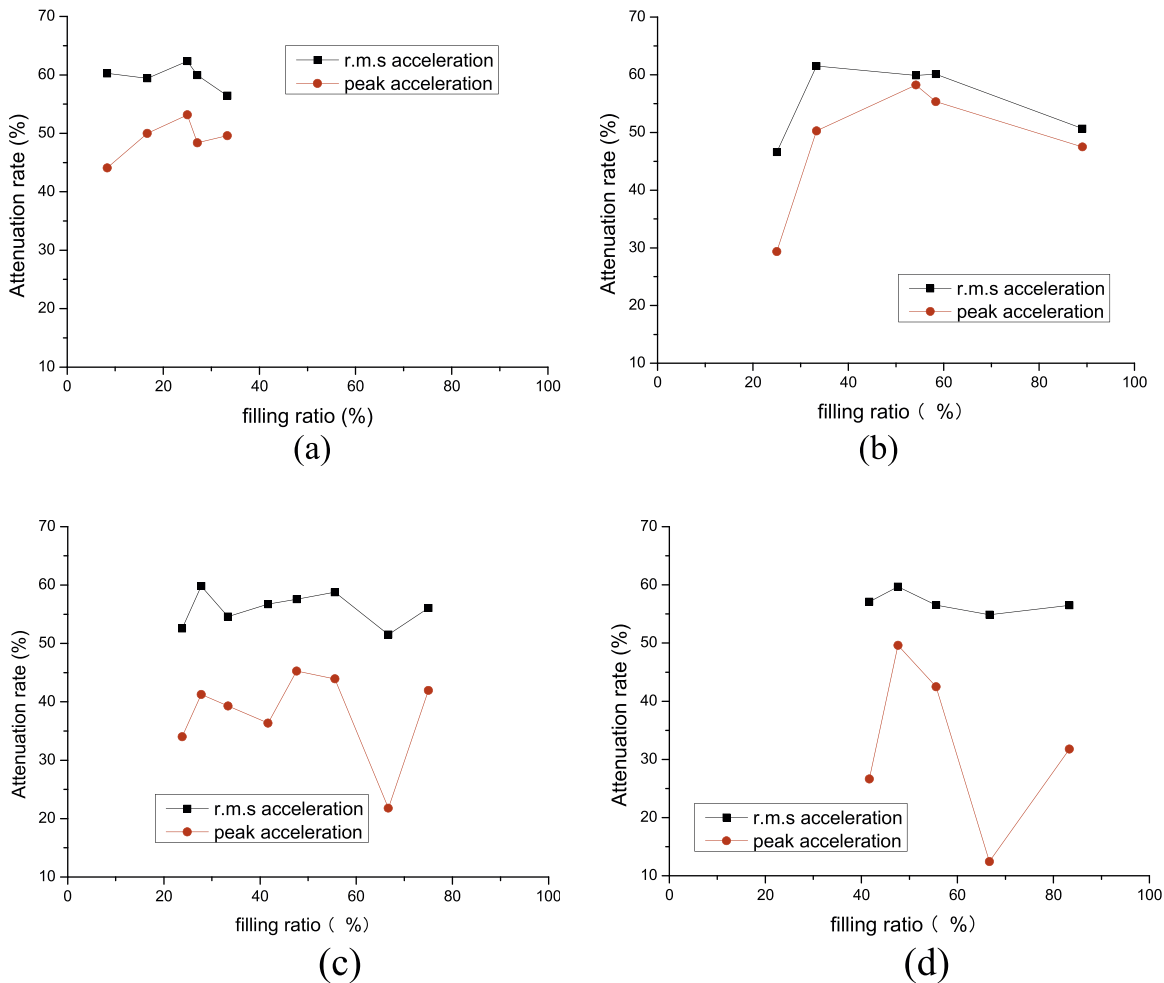


Fig. 3. The effects of filling ratio of particles on the attenuation rate in different cases of mass ratios: (a)  $\mu=0.5\%$ ; (b)  $\mu=1.5\%$ ; (c)  $\mu=2\%$ ; (d)  $\mu=4\%$ .

the vibration control effects when the auxiliary mass ratio is kept constant. In addition, for certain mass ratio cases, there are some peak points in the relationship between the filling ratio and attenuation rate.

To be specific, in the case of  $\mu=0.5\%$ , the attenuation rate increases as the filling ratio increases up to approximately 25%, and then it decreases when the filling ratio is in the range of 25%–40%. In the case of  $\mu=1.5\%$ , the attenuation rate is significant when the filling ratio is around 30% or in the range of 50%–60%. Similarly, in the case of  $\mu=2\%$ , there are three peak points, where the attenuation rate achieves the highest, that is when the filling ratio is approximately 30%, 50–60%, and 80%. Besides, in the case of  $\mu=4\%$ , the attenuation rate is higher when the filling ratio is approximately 50% than that in other filling ratio cases, and when the filling ratio is beyond 70%, the attenuation rate begins to increase.

It can be concluded that the vibration reduction effects are more preferable when the filling ratio is in the range of 20–30%, 50–60% and 80–90%. This is because the distance between particles and the container is changed as the filling ratio of particles varies, which significantly affects the colliding scenarios of the PTMD. When the filling ratio is suitable for particles to move in a plug flow pattern, such as approximately 50%, which can yield considerable effective collisions, the system responses can be significantly reduced.

When the filling ratio is relatively small (20–30%), the particles can move in a relatively large area before collisions. Thus the particles are of high velocity when collisions occur, which makes collisions more effective and results in a higher attenuation rate. However, when the filling ratio is too small (0–20%), it takes a long time for particles to move from one end of the container to the other, and only limited times of collisions take place, decreasing the attenuation performance. When the filling ratio is relatively high (80–90%), more collisions happen during the same period of time compared to the low filling ratio cases on the premise that the particles have sufficient space to move and gain a considerable amount of initial velocity. However, when the filling ratio continually increases (over 90%), the particles have limited space for movement before collisions and even worse, the particles are piled up, so the collisions become less effective than previous situations.

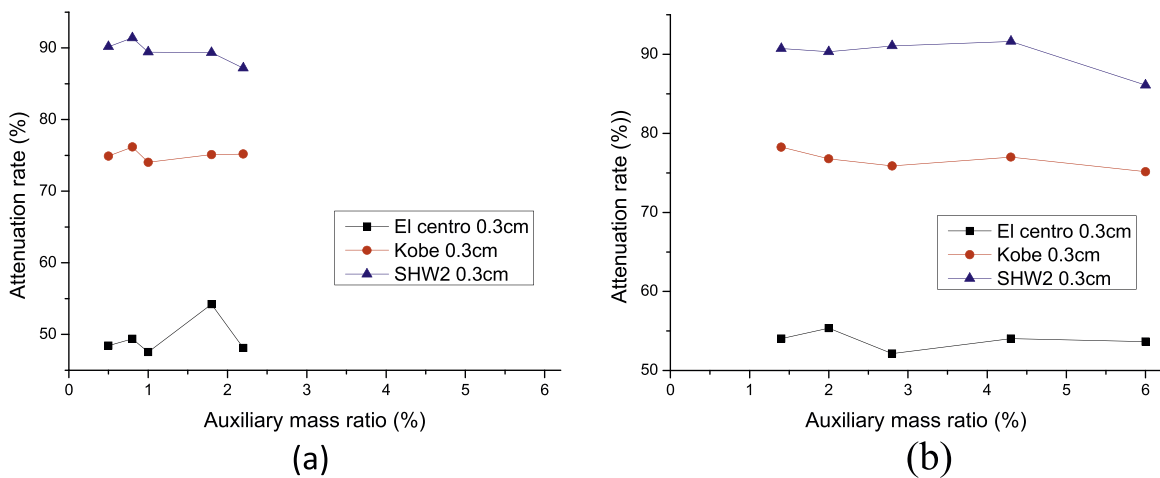


**Fig. 4.** The effects of auxiliary mass ratio on the vibration reduction in different cases of filling ratios: (a) 20–30%; (b) 55–60%.

In conclusion, the filling ratio of particles is a significant parameter that influences the vibration reduction effects of the PTMD system. Therefore, in practical design of the PTMD, the filling ratio should be carefully chosen within these optimum ranges to achieve good vibration control effects.

### 3.2. Effects of auxiliary mass ratio

Researches have suggested that the total auxiliary mass ratio affects the vibration reduction of the particle dampers [24]. Generally speaking, higher values of the mass ratio result in a larger reduction of response, but the reduction is not linearly proportional to the increase of the mass ratio. Moreover, indefinitely increasing the particle mass may not reduce the response any further owing to the piling up phenomena.

It has been observed that the filling ratio of particles plays an important role in vibration control from above analysis. In this part, the influence of the total auxiliary mass ratio on the vibration control when the filling ratio is kept the same or varying in a pretty small range is examined. The mass of the container is kept constant while the total mass of particles is changed by using different types of particles. For example, 7 glass balls, 4 ceramic balls, 5 ceramic balls, 4 steel balls and 14 steel balls are used while their filling ratio of particles are in the range of 20–30%; 26 stainless balls, 10 ceramic balls, 14 ceramic balls, 10 steel balls and 14 steel balls are used while their filling ratio of particles are in the range of 55–60%.

From the parametric study in Section 3.1, the attenuation rates are higher when the filling ratio is around 20–30%, 50–60% and 80–90% than in other filling ratio cases. Fig. 4(a) and (b) show the attenuation rates of the r.m.s acceleration with different auxiliary mass ratios under El Centro wave (0.15 g), Kobe wave (0.15 g) and SHW2 (0.15 g) when the filling ratio is around 20–30% and 55–60%, respectively. It can be found that under a certain input and filling ratio of particles, the attenuate rates present little fluctuation as the auxiliary mass ratio increases, suggesting that the auxiliary mass ratio exerts a slight influence on the vibration reduction under the same filling ratio of particles.

Moreover, it is interesting to find out that the attenuation rate is different under different types of earthquake waves. Actually, the effectiveness of attenuation is significantly influenced by the frequency characteristics of the seismic inputs. The primary frequency of the SHW2 wave is close to the natural frequency of the test structure (1.37 Hz), so the structure vibrated the most under SHW2 wave and the PTMD can give a full play in vibration control. However, the frequencies of the El Centro wave and Kobe wave are concentrated around 0.2 Hz and 0.4 Hz, which largely deviated from the frequency of the test structure. Therefore, the PTMD can achieve the best vibration reduction effects under SHW2 wave than other waves.

Therefore, considering that the vibration control is insensitive to the auxiliary mass ratio provided a suitable filling ratio, the filling ratio of particles should be put in the first place while optimally designing a PTMD.

### 3.3. Effects of particle density

The influence of the particle density on the vibration control effects of the PTMD is investigated by changing the particle material while the total auxiliary mass ratio, the diameter of particles, the container of the PTMD, and the seismic input are kept constant. In the experiment, 7 ceramic balls (density is  $3.56 \text{ g/cm}^3$ ) and 3 steel balls (density is  $7.64 \text{ g/cm}^3$ ) are used when the total auxiliary mass ratio is kept constant as 1.3%, the diameter of particles is 20 mm, and the container size is 60 mm  $\times$  60 mm  $\times$  80 mm. The attenuate rates of both r.m.s and peak accelerations under El Centro wave (0.15 g), Kobe wave (0.15 g) and SHW2 (0.15 g) are shown in Table 1.

**Table 1**

The effects of particle density on the vibration reduction.

| Particle form<br>Material (Density g/cm <sup>3</sup> ) | Particle amount | Filling ratio (%) | Attenuation rate (%) |       |       |       |       |       |
|--|-----------------|-------------------|----------------------|-------|-------|-------|-------|-------|
|  |                 |                   | El Centro            |       | Kobe  |       | SHW2  |       |
|  |                 |                   | r.m.s                | peak  | r.m.s | peak  | r.m.s | peak  |
| Ceramic(3.56)  | 7               | 58.33             | 60.12                | 41.09 | 50.97 | 32.70 | 73.52 | 64.65 |
| Steel(7.64)  | 3               | 25.00             | 56.44                | 29.75 | 46.78 | 26.97 | 59.22 | 51.14 |

It can be observed that the vibration reduction effects for both material cases are pretty good, and their best attenuation rates can achieve 73.52% and 59.22% for r.m.s responses. Furthermore, when the auxiliary mass ratio is the same, the vibration reduction effects are slightly higher when the particles with smaller density are applied. The reason lies in the fact that the amount of particles increases as the density of particles decreases in the case of same auxiliary mass ratio. Consequently, more collisions and friction occur at the same time, which results in increasing dissipated energy.

It is interesting to find that the filling ratios for ceramic case and steel case are 58.33% and 25.00%, respectively. According to the parametric study in Section 3.1, these two filling ratios are both located in the optimum range, which explains the preferable attenuation effects. Moreover, it can be concluded that lower densities of particles are more preferred provided the suitable filling ratio in the optimum design.

In addition, the influence of the particle number on the vibration control effects of the PTMD is investigated by using different particle forms (materials and diameters) while keeping the total auxiliary mass ratio and the container size the same. In the experiment, three forms of particles, including ceramic balls with 20 mm diameter (density is 3.56 g/cm<sup>3</sup>), glass balls with 15 mm diameter (density is 3.00 g/cm<sup>3</sup>), and stainless balls with 10 mm diameter (density is 7.64 g/cm<sup>3</sup>) are used. The mass ratio is kept constant as 1.0% or 1.3% by changing number of particles, and the container size is 60 mm×60 mm×80 mm.

For each mass ratio case, there are three types of particles: ceramic, glass and stainless balls. For a certain type of particles, there are 26 inputs including seismic excitations and stationary random excitations of different magnitudes and characterizations. That is to say, in each mass ratio case, 78 test data can be finally obtained and probability analysis will be conducted among these extensive test data. To be specific, under a certain input, there are 3 test data, which are attenuation rates corresponding to three particle forms. Then 3 test data can be ranked as I-III according to their value of attenuation rates, representing the high, middle and low attenuation rate, respectively. Counting the frequency of occurrence of I-attenuation rate for each material, and then the probability of high attenuation rate for each type of particles can be obtained, as shown in Table 2.

It can be observed that the attenuation rate is not significantly affected with the increase of the particle number. To be specific, when applying 5 ceramic balls and applying 19 stainless balls, whose mass ratio is 1.0%, similar vibration reduction can be achieved. However, when applying 14 glass balls, the attenuation rate is lower. Actually, the most essential parameter behind this phenomenon is the filling ratio of particles. It can be found that the filling ratios of particles in the case of 5 ceramic balls and 19 stainless balls are almost the same, suggesting the similar reduction effects. However, the filling ratio is 65.63% in the case of 14 glass balls, which is difficult to get an optimized damping performance according to the analysis on filling ratio of particles. Similar principles can be obtained from the analysis of 1.3% mass ratio. The vibration reduction is the worst in the case of 19 glass balls, and it is similar in the case of 7 ceramic balls and 26 stainless balls. Therefore, although the particle number increases significantly given the same total mass ratio, the vibration reduction effects are unsatisfied owing to the improper filling ratio.

In short, the filling ratio of particles is most sensitive to the damping performance of the PTMD and therefore should be a primary focus in practical design of the PTMD.

#### 4. Optimum design of PTMD system

As mentioned above, the filling ratio of particles is the key parameter of the PTMD system and the influence of other parameters can be attributed to the filling ratio of particles to some extent. Actually, the filling ratio of particles in multi-particle dampers is an equivalent concept of the gap clearance in single-particle dampers, both of which reflect the colliding behavior between particles and the container during collisions. This paper proposes a simplified numerical simulation method of equating multiple particles to a single particle, which can take the filling ratio of particles into account.

##### 4.1. Numerical simulation method

A simplified analytical solution based on certain equivalent principles is used to simulate the vibration reduction effects of the PTMD. The PTMD can be considered as a particle damper that is suspended to the main structure through strings. Therefore, it is considered as a single pendulum, adding one-degree-of-freedom on the basis of a traditional particle damper. The main focus of the numerical simulation is on the simplification of the multiple-particle damper.

**Table 2**

The effects of particle number on the vibration reduction.

| Mass ratio (%) | Material (Density g/cm <sup>3</sup> ) | Diameter (mm) | Particle amount | Filling ratio (%) | Probability of high attenuation rate (%) |
|----------------|---------------------------------------|---------------|-----------------|-------------------|--|
| 1.0            | Ceramic(3.56)                         | 20            | 5               | 41.67             | 36.63                                    |
|                | Glass(3.00)                           | 15            | 14              | 65.63             | 25.58                                    |
|                | Stainless(7.64)                       | 10            | 19              | 39.58             | 37.79                                    |
| 1.3            | Ceramic(3.56)                         | 20            | 7               | 58.33             | 37.30                                    |
|                | Glass(3.00)                           | 15            | 19              | 89.06             | 21.43                                    |
|                | Stainless(7.64)                       | 10            | 26              | 54.17             | 41.27                                    |

#### 4.1.1. Equivalent method for PTMD

According to the parametric study in Section 3.1, the filling ratio of particles plays a significant role in the vibration control effects of the PTMD. Therefore, particles in the PTMD are equivalent to a single particle by keeping the void volume of the damper the same before and after the equivalence. Besides, the total mass of particles in the PTMD is equal to that of the single particle.

Based on above equivalent principles, the clearance  $d$  of the simplified single-particle damper can be obtained from Eq. (1):

$$\left(\frac{1}{\rho p} - 1\right) \frac{m}{\rho} = \frac{mp}{2\rho} + \frac{\pi}{4} \left(6 \frac{mp}{\pi \rho}\right)^{\frac{2}{3}} d \quad (1)$$

where  $\rho$  is the density of particles,  $\rho_p = V_{spd}/V_{pd}$  is the packing density of the PTMD, and  $V_{spd}, V_{pd}$  is the volume of particles and volume of the container, respectively;  $m$  is the total mass of particles of the PTMD;  $m_p$  is the mass of single particle in the simplified single-particle damper. Based on equivalent principle 2),  $m=m_p$ .

Actually,  $\rho_p$  reflects the filling ratio of particles, which is a determined parameter in the performance of the PTMD.

#### 4.1.2. Equation of motion of PTMD system

For a SDOF structure, based on the equivalent method mentioned above, the structure attaching with a PTMD system can be modeled as a three-degree-of-freedom system, as shown in Fig. 5.  $m$ ,  $k$  and  $c$  are the mass, stiffness and damping coefficient, and the subscript 1,  $c$  and  $p$  represent the main structure, the container and the equivalent single particle, respectively.

The equation of motion of a SDOF structure attaching with a PTMD can be written as Eq. (2):

$$\begin{cases} m_1(\ddot{x}_1 + \ddot{x}_g) + c_1\dot{x}_1 + k_1x_1 - cc(\dot{x}_c - \dot{x}_1) - kc(x_c - x_1) = 0 \\ mc\dot{x}_c + cc(\dot{x}_c - \dot{x}_1) + kc(x_c - x_1) - cpH(y, \dot{y}) - kpG(y) = 0 \\ mp\ddot{x}_p + cpH(y, \dot{y}) + kpG(y) = 0 \end{cases} \quad (2)$$

where  $x$  is the displacement, and  $x_g(t)$  is the displacement of the shaking table;  $y$  is the relative displacement of the simplified particle with respect to the container—i.e.,  $y=x_p-x_c$ .  $kc$  and  $cc$  are used to represent the interaction between the container and the primary structure.  $kc$  can be determined following the basic laws of the simple pendulum:  $k_c=\omega_c^2 m_c=(2\pi f_c)^2 m_c$ ,  $f_c=1/(2\pi)(g/l)^{0.5}$ , where  $l$  is the suspension length of the string, and  $c_c=2m_c\xi_c\omega_c$ .  $kp$  and  $cp$  represent the interaction between the particle and the container:  $k_p=\omega_p^2 m_p$ , and  $c_p=2m_p\xi_p\omega_p$ .  $G(y)$  and  $H(y, \dot{y})$  are used to present the nonlinear behavior between the particle and the container [30].

The vibration reduction effects of the PTMD can be computed by using the MATLAB programming, and Runge-Kutta algorithm is used to solve the ordinary differential equations. Firstly, determine the parameters of the main structure, the PTMD system and excitations, and set the initial motion state of the structure. Secondly, calculate the clearance  $d$  of the simplified particle damper by using Eq. (1). And then, solve the system response, and the vibration control effects of the PTMD can be obtained.

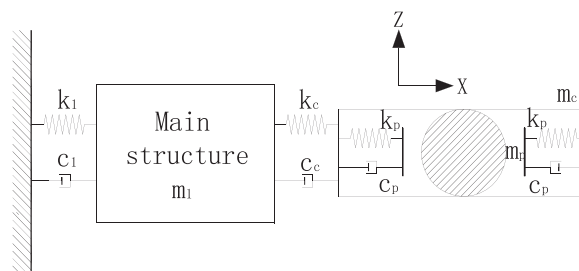


Fig. 5. Schematic diagram of the computational model.

#### 4.2. Validation of simulation method

In order to validate the rationality and accuracy of the numerical simulation method proposed in Section 4.1, the numerical analysis is conducted to simulate the experimental conditions.

##### 4.2.1. Parameter determination

The size of the container is 60 mm × 60 mm × 80 mm, and it is filled with 26 stainless steel balls with 10 mm diameter (the density is 7.64 g/cm<sup>3</sup>). El Centro and Kobe wave that are recorded from the shaking table tests are applied to the main structure. The initial displacement and velocity are set as zero for convenience. The parameters used in the numerical simulation are listed in Table 3.

The damping ratio of the container is determined by trial calculations as it is hard to test in the experiment. It can be found that the vibration responses of the structure do not change significantly when the damping ratio of the container is lower than 0.05. That is to say, this parameter is insensitive to the system response as long as the value being less than 0.05. Therefore the damping ratio of the container is finally determined as 0.05.

According to Masri and Ibrahim [31], when  $\omega_3 \geq 20\omega_1$ , it can properly simulate the interaction between the particles and the container. Therefore, the circular frequency  $\omega_3$  is set as  $20\omega_1$ .

The damping ratio  $\xi_3$  is related to the coefficient of restitution  $e$  [30]. The coefficient of restitution  $e$  is set as 0.25, so the damping ratio  $\xi_3$  is determined as 0.375. Moreover, the time step is set as 0.002 s.

##### 4.2.2. Comparison of numerical and experimental results

Fig. 6 shows both the calculated and experimental results for the acceleration and displacement time histories on the top of the test structure with the PTMD under El Centro wave. They generally agree well with each other, but there are deviations between them at some intervals. On one hand, the deviation may be caused by the initial acceleration and displacement value being zero. As the calculation goes on, the influence of the initial motion state on the system response decreases gradually. On the other hand, the PTMD performs nonlinearly under the seismic excitations, but the proposed numerical simulation simplifies the highly nonlinear behavior of particles to a certain extent. For example, the collisions between particles are not considered in the numerical simulation. However, this method still captures the nonlinear behavior between the particle and the container, which is the most important control force for the primary structure. Therefore, it can provide an estimation of the controlling force with reasonable accuracy.

In addition, the comparison of the calculated and experimental results for the peak and r.m.s value of acceleration response on the top of the test structure with the PTMD under El Centro and Kobe wave is listed in Table 4. It can be observed that the experimental and calculated results for the peak value of response agree soundly, and the errors for the r.m.s value of responses can be limited in an acceptable range. Actually, the acceleration peak value is an important controlling index in design of buildings which are regulated in the Chinese code, since excessive acceleration values may cause discomfort feeling of the occupants. As a result, the simplified numerical simulation method proposed in this paper can estimate the acceleration peak and r.m.s value properly.

In conclusion, the proposed approximate analytical solution based on the concept of an equivalent single-particle damper can achieve a reasonably accurate estimate of the dynamic behavior of the structure attaching with a PTMD, especially for the peak values of the structural responses. Moreover, this method has certain practical value in actual design of the PTMD owing to its simple principle and convenient operation.

Besides, this simplified method also proved to be feasible in predicting the motion trends with an acceptable accuracy and providing reasonably accurate estimates of the maximum response when the PTMD applied to a five-storey steel structure [30].

#### 4.3. Guidelines for optimization of PTMD

It is admitted that to precisely simulate the performance of the structure attaching with a PTMD under seismic excitations, further comprehensive studies and more accurate numerical methods are needed, especially considering the influence of collisions between particles. However, this equivalent analytical solution has certain accuracy in estimating the performance of the PTMD. Furthermore, this method highly considers the parameter of filling ratio of particles, which is corresponding to the influencing rules from the experimentally parametric analysis. Thus it can be used for the preliminary design of an efficient PTMD system.

**Table 3**

Values of system parameters.

|                            | Mass(kg) | Circular frequency (rad/s) | Damping ratio |
|----------------------------|----------|----------------------------|---------------|
| Main structure             | 7.6      | 8.608                      | 0.032         |
| Container                  | 0.128    | 8.608                      | 0.05          |
| Equivalent single particle | 0.832    | 172.16                     | 0.375         |

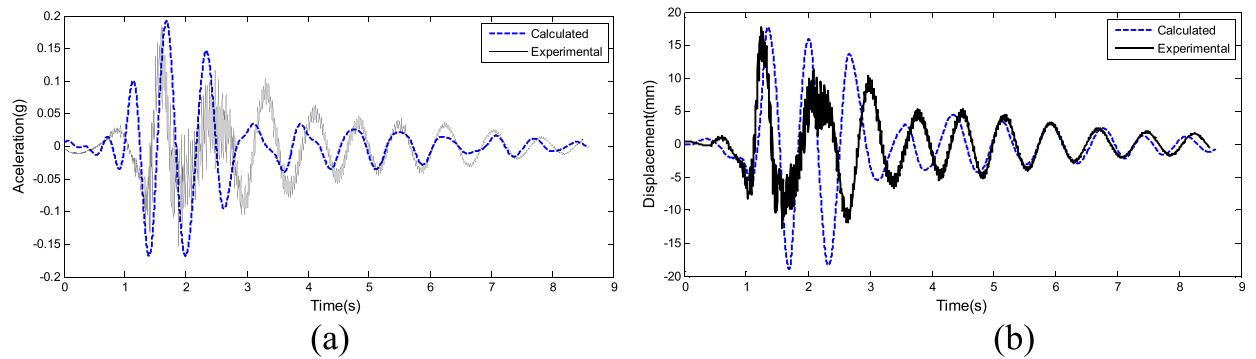


**Fig. 6.** Response time histories on the top of the test structure with the PTMD under El Centro wave: (a) acceleration; (b) displacement.

**Table 4**

Comparison of the calculated and experimental results for the peak and r.m.s value of acceleration response on the top of the test structure with the PTMD.

| Input     | Particle amount | Particle material | Peak value of acceleration |                        |           | r.m.s value of acceleration |                        |           |
|-----------|-----------------|-------------------|----------------------------|------------------------|-----------|-----------------------------|------------------------|-----------|
|           |                 |                   | Calculation ( $m/s^2$ )    | Experiment ( $m/s^2$ ) | Error (%) | Calculation ( $m/s^2$ )     | Experiment ( $m/s^2$ ) | Error (%) |
| El Centro | 4               | Steel             | 2.6024                     | 2.5645                 | 1.46      | 0.5696                      | 0.5378                 | 5.58      |
|           | 5               | Steel             | 2.6049                     | 2.6949                 | -3.46     | 0.5582                      | 0.5538                 | 0.79      |
|           | 19              | Stainless         | 1.9674                     | 1.9299                 | 1.90      | 0.5771                      | 0.5494                 | 4.81      |
|           | 26              | Stainless         | 1.8833                     | 1.8259                 | 3.05      | 0.5763                      | 0.5607                 | 2.71      |
|           | 4               | Steel             | 3.5215                     | 3.5518                 | -0.86     | 0.5056                      | 0.5377                 | -6.34     |
|           | 5               | Steel             | 3.7400                     | 3.7354                 | 0.12      | 0.5345                      | 0.5799                 | -8.49     |
|           | 19              | Stainless         | 3.8869                     | 3.8562                 | 0.79      | 0.5245                      | 0.5751                 | -9.64     |
|           | 26              | Stainless         | 3.6410                     | 3.7484                 | -2.95     | 0.4983                      | 0.5435                 | -9.07     |

Given the structural characteristics of the primary system with the mass of  $M$ , the diameter of particles  $D_p$ , and the excitation, the steps that one can follow to design an optimum PTMD with favorable vibration reduction effects attached to a lightly damped primary system are summarized as below:

- 1) Determine the material of particles. According to the parametric analysis about effects of the particle density on the damping performance of the PTMD in Section 3.3, the particles with smaller density  $\rho$  can be used.
- 2) Considering the specific engineering conditions, preset a proper range of total auxiliary mass ratio  $\mu$  based on scientific researches and practical experiences. For example, in area of civil engineering, an auxiliary mass ratio of 0.5–3% is commonly used.
- 3) Considering the practical requirements, preset the mass ratio of the container to particles  $\mu'$ . According to the reference [19], when the auxiliary mass ratio of the damper to the primary structure is constant, the vibration reduction effects increase as the mass ratio of the container to particles decrease. Therefore, smaller mass of the container is preferred.
- 4) Determine an optimum filling ratio of particles  $\alpha$  based on experimental parametric analysis mentioned above. It is suggested that  $\alpha$  plays a significant role in the vibration control of the PTMD, and when  $\alpha$  is located in the ranges of 20%–30%, 50%–60% and 80%–90%, the PTMD is more effective in attenuating the vibration.
- 5) For a given auxiliary mass ratio  $\mu$  and filling ratio  $\alpha$ , by using the analytical method proposed in Section 4.1, solve the system response. When  $\mu$  is known, the total mass of particles  $m$  and the mass of the container  $m_c$  can be obtained that  $m = \mu \times M/(1 + \mu')$  and  $m_c = \mu' \times m$ . Then, the mass of the equivalent single particle damper  $m_3$  can be obtained, which equals to  $m$  according to equivalent principles. Thus, as the Eq. (1) suggests, the relationship between the clearance of the single particle damper  $d$  and  $\alpha$  can be obtained, as shown in Eq. (3) which is of the form:

$$d = f(\alpha) \quad (3)$$

That is to say, for a certain filling ratio  $\alpha$ , there is a clearance  $d$  corresponding to it. Thus, the dimensionless response  $x/\sigma$  of the primary system attached with a single particle damper can be computed by following steps in Section 4.1.2, as shown in Eq. (4). This result can be approximately considered as the response of the primary system attached with a PTMD of the same mass and same empty volume.

$$x/\sigma = g(d, \alpha) \quad (4)$$

where  $x$  and  $\sigma$  are the response of the primary system attached with a single particle damper and that of the system with no dampers, respectively.

- 6) By changing the values of mass ratio  $\mu$  chosen in step 2), determine an optimum  $\mu$  corresponding to the determined filling ratio  $\alpha$ , where the lowest  $x/\sigma$  can be achieved. Then,  $m$  and  $m_c$  can be obtained.
- 7) Using the relationship  $m = N\pi D p^3 \rho / 6$ , the amount of particles  $N$  in the PTMD can be obtained.
- 8) Using the relationship  $\alpha = N/N_0$  and  $N_0$  is the maximum amount of particles that are available in one layer of the PTMD, and considering the mass of the container  $m_c$ , determine the material and dimensions of the container.

If the response of the structure is not satisfactory, alternative values for optimum filling ratio of particles  $\alpha$  can be selected and the above procedure is repeated.

## 5. Application

The experiment on a one-storey steel structure described in [Section 2](#) was conducted to preliminarily investigate the effects of the particle tuned mass damper when it was used to control the vibration. However, as the high-rise buildings, especially the super-tall buildings rapidly develop in modern society, new passive control devices, such as the PTMD, are urgently expected and demanded to attenuate their responses. Therefore, shaking table tests on multi-storey buildings attached with a PTMD are necessary, which could help further the understanding of the physical mechanism of such a device and advance its application in practical engineering projects. Besides, the large-scale shaking table test has more engineering reference than that tested one-storey frame.

### 5.1. An optimum PTMD

The optimization design process for a PTMD system proposed above are demonstrated by application to a 5-storey steel frame attached with a PTMD on its top. The primary structure has the total mass of 6000 kg, and the total height is 5.48 m, as shown in [Fig. 7\(a\)](#). The plane and elevation dimensions are demonstrated in [Fig. 7\(b\)](#). The frame columns are made of high-strength steel plates (Q690) with width  $\times$  length  $\times$  height dimensions of 15 mm  $\times$  180 mm  $\times$  1060 mm. The slabs are made of steel plates (Q345) with a thickness of 30 mm. The first three frequencies of the primary structure are 1 Hz, 3 Hz and 5 Hz, respectively.

The preliminary optimization process of the PTMD is shown as follows:

- 1) Considering the configuration and mass of the primary structure, steel balls with diameter of 51 mm are selected.
- 2) The auxiliary mass ratio  $\mu$  is preliminarily set in range of 1–2.5%.
- 3) Set the relationship  $m_c=0.4 \times m$ .
- 4) Take the optimum filling ratio of particles  $\alpha$  of 50% as an example.

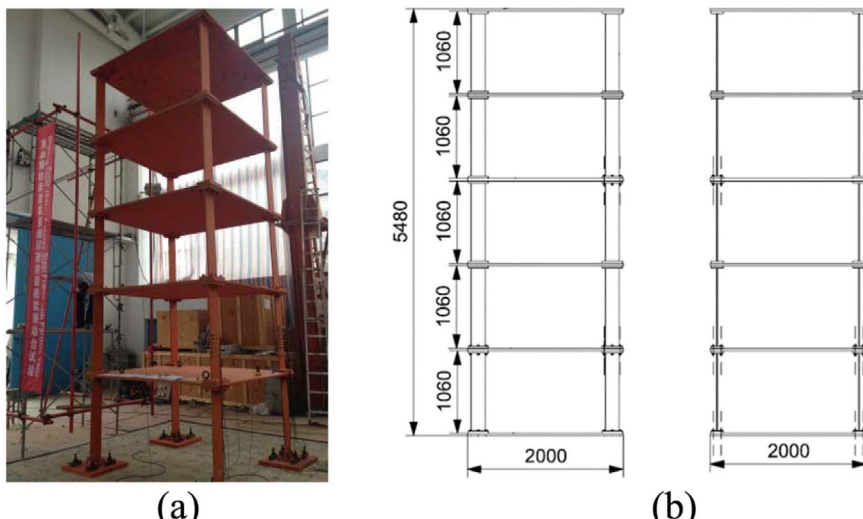


**Fig. 7.** Configuration of the test structure: (a) photo of the experimental model; (b) plane and elevation dimensions.

- 5) When the filling ratio of particles  $\alpha$  equals to 50%,  $x/\sigma$  ( $x$  represents the peak and r.m.s displacement, respectively) under different mass ratios are shown in Fig. 8.
- 6) It can be seen from Fig. 8 that when the value of mass ratio  $\mu$  is in range of 2.3–2.4%,  $x/\sigma$  for both peak and r.m.s displacements get the lowest value, which suggests the highest reduction of structural responses. Therefore, the optimum mass ratio  $\mu$  is determined as approximately 2.35%. Then, the total mass of particles is computed as

$$m = \mu \times M/(1 + \mu') = 0.0235 \times 6000/(1 + 0.4) = 100\text{kg}$$

$$mc = \mu' \times m = 0.4 \times 100 = 40\text{kg}$$

- 7) The total amount of particles in the PTMD can be obtained from

$$N = 6 \times m/\rho/Dp^3/\pi = 6 \times 100/7644/0.051^3/\pi = 189$$

Considering the limitations of the plane dimensions of the primary structure, the particles are designed to place in two layers. In addition, to increase the collisions between particles and the wall of the container, the PTMD is designed as a multi-unit damper. For each layer, the container is divided into 6 small cavities and the particles are equally put into them. Therefore, the amount of particles in each small cavity is about 15.

- 8) The maximum amount of particles in one small cavity is thus 30. Finally, the container is designed to be made of wooden plates with a thickness of 4 cm. The outer dimensions are 1000 mm×640 mm×300 mm, and the inner dimension of each small cavity is 288 mm×283 mm×120 mm. The total mass of the container is 39.345 kg.

## 5.2. Experimental validation

Based on the parameters of the optimum PTMD above, several experimental cases of different types of particles are designed to thoroughly explore the reduction laws of the PTMD, and the detailed analysis is presented in [30].

Meanwhile, the advantages of the optimum PTMD in vibration control can be exhibited by comparing with other PTMDs according to experimental results. For example, the cases of 1.19% and 1.73% auxiliary mass ratio, which means 60 and 120 particles equally placed into 12 cavities, respectively, are compared with the optimum case (2.26% auxiliary mass ratio), and Table 5 shows their attenuation rates of both the r.m.s and peak displacements under El Centro Wave (0.1 g). It can be observed that the optimum PTMD dose have more efficiency in attenuating the responses, especially for the peak displacement response, which indicates the feasibility and reliability of the optimization process proposed in Section 4.3.

In addition, it is interesting to notice that the attenuation rate in the case of 1.73% is equal or even slightly lower than that in the case of 1.19%. Generally speaking, the vibration control effects get better as the mass of particles increases because adding particles can lead to more collisions and thus dissipate more energy. Actually, the low attenuation rate in a relatively high mass ratio case can be attributed to an improper filling ratio of particles. When the mass ratio is 1.73%, the corresponding filling ratio is about 34%, which is outside the optimum range of the filling ratio, as suggested in Section 3.1. Thus, the positive influence of the increasing mass of particles to the vibration control could be counteracted by the negative influence of the improper arrangement of particles. This again strengthens the principle that the filling ratio of particles in the PTMD system plays a vital role.

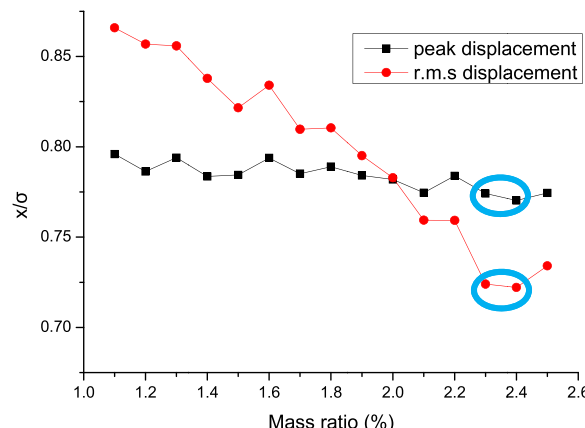


Fig. 8. Vibration control effects of the PTMD under different mass ratios ( $\alpha=50\%$ ).

**Table 5**

Comparison of attenuation rates of different PTMDs.

| Mass ratio (%) | Particle amount | Filling ratio (%) | Attenuation rate (%) |       |
|----------------|-----------------|-------------------|----------------------|-------|
|                |                 |                   | r.m.s                | peak  |
| 1.19           | 60              | 17%               | 61.63                | 17.35 |
| 1.73           | 120             | 34%               | 61.56                | 16.59 |
| 2.26           | 180             | 50%               | 63.40                | 22.65 |

Although the filling ratio of particles exerts an important influence in the behavior of the PTMD and other parameters are related to the filling ratio to some extent according to current researches, the physical mechanism of the PTMD is a pretty complicated issue that involves multiple energy dissipation methods. In order to have a deeper understanding of the contribution of each part and the interaction among them, more fining and accurate theoretical, experimental and numerical analysis should be conducted. As for the optimal design of the PTMD, a more comprehensive procedure that can conveniently takes several key parameters into account is expected to better guide the engineering practice.

## 6. Conclusions

This paper presents the experimental investigation of the seismic vibration control effects of a new type of passive control device, the particle tuned mass damper, which combines the advantages of both tuned mass damper and particle damper. Free vibration tests and small-scale shaking table tests are conducted on a one-storey steel frame attached with a PTMD on its top. Thorough parametric analysis based on the experimental results explores the influencing laws of some key parameters, including the filling ratio of particles, auxiliary mass ratio and particle density. In addition, a numerical model of an equivalent simplified single-particle damper is proposed for optimally designing a PTMD. A case study of the preliminary optimization design of the PTMD attached to a multi-storey building following the proposed steps is presented and shows a satisfactory result. Based on the experimental and numerical analysis, the following conclusions can be drawn:

- 1) The new PTMD can significantly reduce both r.m.s and peak responses under free vibration and seismic excitations, which suggests the good efficiency of the PTMD in vibration control.
- 2) According to parametric study, the filling ratio of particles plays the most important role in the working mechanism of the PTMD. When the filling ratio is in range of 20–30%, 50–60% and 80–90%, the highest attenuation level is most likely obtained. The auxiliary mass ratio does not significantly influence the attenuation rate in cases of an optimum filling ratio. In addition, the vibration control effects decrease as the density of particles increases provided a suitable filling ratio.
- 3) The numerical simulation results show a favorable agreement with the experimental results, thus the proposed equivalent analytical method can be used to estimate the damping performance of the PTMD and improve the understanding of the physical mechanism of the PTMD.
- 4) Based on the experimentally parametric study, the filling ratio of particles should be put in the first place in the optimum design of the PTMD. A series of guidelines for optimally designing a preferable PTMD are concluded as follows: determining the particle density and a lower density is preferred; setting the range of the auxiliary mass ratio according to engineering practice; choosing a proper filling ratio that is in range of 20–30%, 50–60% or 80–90%; using the proposed analytical simulation method to determine the optimum mass ratio, corresponding to the determined filling ratio of particles; deciding the material and dimensions of the container. Furthermore, the proposed simplified numerical method is closely related to the filling ratio of particles and thus can serve as a reliable channel for the preliminary optimization design of the PTMD.

In conclusion, a large reduction of structural responses can be achieved by attaching a lightweight PTMD on the top of the primary structure. Through collisions and frictions between particles, and that between particles and the container, and tuning frequency by the added masses, the vibration is attenuated significantly, which shows a good prospect in the application of civil engineering. The guidelines also offer a feasible example for the optimum design of the PTMD.

## Acknowledgements

Financial support from the National Natural Science Foundation of China through grant 51478361 is highly appreciated. The work is also supported by the Fundamental Research Funds for the Central Government Supported Universities.

## References

- [1] Z. Lu, X.Y. Chen, X.L. Lu, Z. Yang, Shaking table test and numerical simulation of an RC frame-core tube structure for earthquake-induced collapse, *Earthq. Eng. Struct. Dyn.* 45 (9) (2016) 1537–1556.
- [2] J.M. Kelly, R.J. Skinner, Mechanisms of energy absorption in special devices for use in earthquake resistant structures, *Bull. N. Zeal. Soc. Earthq. Eng.* 5 (3) (1972) 63–88.

- [3] Y. Zhou, C.Q. Zhang, X.L. Lu, Seismic performance of a damping outrigger system for tall buildings, *Struct. Control Health Monit.* (2016), <https://doi.org/10.1002/stc.1864>.
- [4] Z. Lu, Y.L. Yang, X.L. Lu, C.Q. Liu, Preliminary study on the damping effect of a lateral damping buffer under a debris flow load, *Appl. Sci.* 7 (2) (2017) 201.
- [5] K.S. Dai, J.Z. Wang, R.F. Mao, Z. Lu, S.E. Chen, Experimental investigation on dynamic characterization and seismic control performance of a TLPD system, *Struct. Des. Tall Spec. Build.* (2016), <https://doi.org/10.1002/tal.1350>.
- [6] Z. Lu, X.L. Lu, W.S. Lu, S.F. Masri, Shaking table test of the effects of multi-unit particle dampers attached to an MDOF system under earthquake excitation, *Earthq. Eng. Struct. Dyn.* 41 (5) (2012) 987–1000.
- [7] Z. Lu, X.Y. Chen, X.W. Li, P.Z. Li, Optimization and application of multiple tuned mass dampers in the vibration control of pedestrian bridges, *Struct. Eng. Mech.* 62 (1) (2017) 55–64.
- [8] X.L. Lu, K. Ding, W.X. Shi, D.G. Weng, Tuned mass dampers for human-induced vibration control of the Expo Culture Centre at the World Expo 2010 in Shanghai, China, *Struct. Eng. Mech.* 43 (5) (2012) 607–621.
- [9] T. Haskett, B. Breukelman, J. Robinson and J. Kottellenberg, Tuned mass dampers under excessive structural excitation [J]. Report of the Motioneering Inc., Guelph, Ontario, Canada NIK IB8, 2004.
- [10] B. Fitzgerald, B. Basu, S.R.K. Nielsen, Active tuned mass dampers for control of in-plane vibrations of wind turbine blades, *Struct. Control Health Monit.* 20 (12) (2013) 1377–1396.
- [11] C.M. Casado, D.S. Jesus, I.M. Diaz, A. Lorenzana, Vibration control of pedestrian bridges, *Dyna* 86 (3) (2011) 318–327.
- [12] H. Tanaka, C.Y. Mak, Effect of tuned mass dampers on wind induced response of tall buildings, *J. Wind Eng. Ind. Aerodyn.* 14 (s1–3) (1983) 357–368.
- [13] J.F. Clinton, The observed wander of the natural frequencies in a structure, *Bull. Seism. Soc. Am.* 96 (1) (2006) 237–257.
- [14] Z. Lu, D.C. Wang, P.Z. Li, Comparison study of vibration control effects between suspended tuned mass damper and particle damper, *Shock Vib.* 33 (2) (2014) 233–243.
- [15] Z. Lu, X.L. Lu, W.S. Lu, S.F. Masri, Experimental studies of the effects of buffered particle dampers attached to a multi-degree-of-freedom system under dynamic loads, *J. Sound Vib.* 331 (9) (2012) 2007–2022.
- [16] Z. Lu, S.F. Masri, X.L. Lu, Parametric studies of the performance of particle dampers under harmonic excitation, *Struct. Control Health Monit.* 18 (1) (2011) 79–98.
- [17] L. Hu, Y.G. Shi, Q.L. Yang, G.B. Song, Sound reduction at a target point inside an enclosed cavity using particle dampers, *J. Sound Vib.* 384 (8) (2016) 45–55.
- [18] W.M. Yan, W.B. Xu, J. Wang, Y.J. Chen, Experimental research on the effects of a tuned particle damper on a viaduct system under seismic loads, *J. Bridge Eng.* 19 (3) (2014) 04013004-1–04013004-10.
- [19] Z. Lu, D.C. Wang, S.F. Masri, X.L. Lu, An experimental study of vibration control of wind-excited high-rise buildings using particle tuned mass dampers, *Smart Struct. Syst.* 18 (1) (2016) 93–115.
- [20] Z. Lu, D.C. Wang, Y. Zhou, Experimental parametric study on wind-induced vibration control of particle tuned mass damper on a benchmark high-rise building, *Struct. Des. Tall Spec. Build.* (2017), <https://doi.org/10.1002/tal.1359>.
- [21] R.E. Roberson, Synthesis of a nonlinear dynamic vibration absorber, *J. Franklin Inst.* 254 (3) (1952) 205–220.
- [22] N. Wierschem, S. Hubbard, J. Luo, L. Fahnestock, B. Spencer, D. Quinn, D. McFarland, A. Vakakis, L. Bergman Experimental blast testing of a large 9-story structure equipped with a system of nonlinear energy sinks, ASME International Design Engineering Technical Conferences and Computers and Information in Engineering Conference, Portland: 2013.
- [23] N.E. Wierschem, D.D. Quinn, S.A. Hubbard, M.A. Al-Shudeifat, D.M. McFarland, J. Luo, L.A. Fahnestock, B.F. Spencer, A.F. Vakakis, L.A. Bergman, Passive damping enhancement of a two-degree-of-freedom system through a strongly nonlinear two-degree-of-freedom attachment, *J. Sound Vib.* 331 (25) (2012) 5393–5407.
- [24] A. Papalou, S.F. Masri, Performance of particle dampers under random excitation, *J. Vib. Acoust.* 118 (4) (1996) 614–621.
- [25] Z.W. Xia, X.D. Liu, Y.C. Shan, X.H. Li, Coupling simulation algorithm of discrete element method and finite element method for particle damper, *J. Low. Freq. Noise Vib. Act. Control* 28 (3) (2009) 197–204.
- [26] Z. Lu, X.L. Lu, S.F. Masri, Studies of the performance of particle dampers under dynamic loads, *J. Sound Vib.* 329 (26) (2010) 5415–5433.
- [27] Z. Lu, S.F. Masri, H.J. Jiang, Discrete element method simulation and experimental validation of particle damper system, *Eng. Comput.* 31 (4) (2014) 810–823.
- [28] D.Q. Wang, C.J. Wu, A novel prediction method of vibration and acoustic radiation for rectangular plate with particle dampers, *J. Mech. Sci. Technol.* 30 (3) (2016) 1021–1035.
- [29] M. Sanchez, C.M. Carlevaro, Nonlinear dynamic analysis of an optimal particle damper, *J. Sound Vib.* 332 (8) (2013) 2070–2080.
- [30] Z. Lu, X.Y. Chen, D.C. Zhang, K.S. Dai, Experimental and analytical study on the performance of particle tuned mass dampers under seismic excitation, *Earthq. Eng. Struct. Dyn.* 46 (5) (2017) 697–714.
- [31] S.F. Masri, A.M. Ibrahim, Response of the impact damper to stationary random excitation, *J. Acoust. Soc. Am.* 53 (1) (1973) 200–211.